A MAGNETIC ISOLATION AND POINTING SYSTEM FOR THE ASTROMETRIC TELESCOPE FACILITY*

William Hibble and
Patrick J. Wolke
Satellite Systems Division
Honeywell Inc.

Marcie Smith
NASA Ames Research Center

SUMMARY

The astrometric telescope facility (ATF), a 20-meter telescope designed for long-term detection and observation of planetary systems outside of the solar system, is scheduled to be a major user of the Space Station's payload pointing system (PPS) capabilities. However, because the ATF has such a stringent pointing stability specification (as low as 0.01 arcsec error over the frequency range from 5 to 200 hertz) and requires +/- 180-degree roll rotation around the telescope's line of sight, the ATF's utilization of the PPS requires the addition of a mechanism or mechanisms to enhance the basic PPS capabilities. This paper presents the results of a study conducted to investigate the ATF pointing performance achievable by the addition of a magnetic isolation and pointing (MIPS) system between the PPS upper gimbal and the ATF, and separately, by the addition of a passive isolation system between the Space Station and the PPS base. In addition, the study has produced requirements on magnetic force and gap motion as a function of the level of Space Station disturbance. These results have been used to support the definition of a candidate MIPS.

Pointing performance results from the study indicate that an MIPS can meet the ATF pointing requirements in the presence of a PPS base transitional acceleration of up to 0.018g, with reasonable restrictions placed on the isolation and pointing bandwidths. By contrast, the passive base isolator system must have an unrealistically low isolation bandwidth on all axes (less than 0.1 hertz) to meet ATF pointing requirements.

The candidate MIPS, described in this paper, is based on an assumed base translational disturbance of 0.01g. The system fits within the available annular region between the PPS and ATF while meeting power and weight limitations and providing the required payload roll motion. Payload data and power services are provided by noncontacting transfer devices.

---

*This work was performed for NASA Ames Research Center under Contract No. NAS2-12525.

INTRODUCTION

The astrometric telescope facility (ATF) is a single-mirror optical telescope whose primary purpose is to search for extrasolar planetary systems (ref. 1). The ATF will measure the positions of selected nearby stars relative to sets of distant reference stars with an accuracy of 10 microarcseconds. By analyzing the motion of these stars over several years, it will be possible to infer the presence or absence of planetary systems.

The accuracy of the measurement is determined by the requirement to detect Uranus/Neptune-size planets orbiting solar-size stars up to 10 parsecs from Earth. To make this measurement, the target star and reference stars' signals in the focal plane are modulated by passing the collected light through a moving grating, called a Ronchi ruling. The ruling modulation frequency can be commanded between 10 and 100 hertz.

The ATF is designed to be an attached payload on the Space Station (SS) and uses many SS services. Because the mission span is long (20 years), the advantages of the low operating costs associated with the SS are great. As well as using the station power and data systems, the ATF requires use of one of the SS PPS for orienting the telescope relative to the station. The PPS will provide three-axis pointing with 1 arcmin pointing accuracy and 15 arcsec jitter.

The telescope design is shown in figure 1. The ATF has a 1.25-meter-diameter paraboloid mirror and a focal ratio of 13. The tube, itself, is 1.85 meters in diameter and 20 meters long, including the sun shade. The mass of the telescope is 3340 kilograms. The telescope uses about 1.0 kilowatts power continuously and has a 1.75 Mbps downlink data rate.

Although the dimensions of the PPS allow for motion of the telescope to view all stars, the PPS, alone, will not satisfy the pointing and isolation requirements of the ATF. The ATF requires 1 arcsec pointing accuracy and has stringent frequency-dependent jitter requirements. The most severe requirement is to control the jitter of the image at the Ronchi ruling to 0.01 arcsec in a bandwidth between one half and two times the ruling frequency (5 - 200 hertz). For frequencies below 5 hertz, the jitter must be less than 1 arcsec; for frequencies above 200 hertz, it must be less than 0.1 arcsec.

Space Station disturbance accelerations and motions are expected to generate PPS pointing error levels, even for a center-of-gravity mounted payload, that are significantly above ATF specifications. Additionally, although the PPS provides three axes of active pointing, the telescope still must be able to roll +/- 180 degrees to allow measurement of star positions in two dimensions. To meet these requirements, the ATF preliminary design concept places an annular vibration isolation/vernier pointing system between the ATF and the PPS, which includes a roll mechanism to position the telescope about the line of sight.

This paper presents the results of a study which had as its primary objective the determination of ATF pointing performance achievable by adding a magnetic isolation and pointing system (MIPS) between the PPS and the ATF. The MIPS provides a noncontacting interface between the PPS gimbal system and the ATF. Magnetic actuators, similar to the one illustrated in figure 2, are used to point the ATF inertially and to isolate the ATF from PPS translational motions. The stators of the actuators are connected to the PPS; the armatures are attached to the ATF.

The magnetic system pointing performance results were primarily parametric in nature, defining pointing performance as a function of the level of input disturbance from the Space Station and of allowable control bandwidths, for both pointing and isolation functions.

The secondary objections of the ATF study include: 1) the comparison of the MIPS performance with that obtained by adding a passive isolation system to the base of the PPS and, 2) the definition of a candidate MIPS which would serve as a basis for establishing system power, weight, and size budgets. The proposed magnetic system design is based on Honeywell's activities over the past decade in developing similar MIPS for space and ground test applications (ref. 2-16).

SPACE STATION DISTURBANCE CHARACTERIZATION

The major sources of ATF pointing errors are expected to be the SS motions and accelerations generated at the base of the PPS. The translational accelerations at the PPS control center (intersection of the gimbal axes in figure 1), resulting from both translational and angular accelerations at the PPS base, produce a disturbance torque to the PPS control loop that is proportional to the offset between the control point and the payload center of gravity. Similarly, the SS rotational motion is coupled into the PPS control loops by the gimbal bearing friction and by any fluid couplings or electrical cabling required for the payload.

By adding an isolator below the PPS, the disturbance levels into the pointing loops are reduced. Alternatively, the MIPS, by adding a noncontacting interface between the PPS and the ATF, removes the effect of the rotational coupling to the payload, attenuates the translational disturbances transmitted through the PPS, and makes payload pointing control very insensitive to the gimbal-to-payload center of gravity, since the magnetic system provides the pointing control. In addition, the magnetic system isolates the payload from disturbances produced by the PPS itself.

Ideally, models of the SS and its disturbance forces and torques would be used to generate an estimate of the PPS base motions and accelerations. However, the Space Station is not defined well enough to allow this option. Thus, disturbances at the PPS base were assumed to consist of discrete spectrums of sinusoidal rotations and translational accelerations.

Meaningful study performance results were obtained by limiting the spectrum to two frequencies, one above 5 hertz and the other below 5 hertz. The two frequencies were selected to provide worst-case pointing errors in these respective frequency ranges. In this ATF study, a conservative value of 0.01g translation acceleration magnitude was assumed for the linear disturbance levels, both below and above 5 hertz. For rotational disturbance, a one-arcmin rotational magnitude was used.

PASSIVE BASE ISOLATOR COMPARISON

Evaluation of ATF pointing performance, assuming a PPS with passive base isolation, was performed with a simple planar model. The model included the PPS azimuth and elevation gimbals and assumed the cross-elevation gimbal would be replaced with a roll mechanism. The PPS pointing loop bandwidth was considered limited to 5 radians per second by the lowest gimbal structural mode of 5 hertz. The isolator system was comprised of spring-fluidic damper elements.

Results of the study indicated that to meet the ATF pointing requirements with the specified disturbance inputs, the isolation bandwidth had to be extremely low, (less than 0.3 radians per second. Such an isolator would require an extremely large stroke (over 0.3 meter). Since the estimated upper limit on actuator deflection for a reasonably sized isolator element of the space telescope reaction wheel isolator variety (ref. 17) is about 0.03 meter, no additional hardware studies with this configuration were pursued, and emphasis was placed on the MIPS.

MAGNETIC ISOLATION AND POINTING PERFORMANCE MODEL

To define a model of the PPS-magnetic system, some basic assumptions about the system's physical characteristics and operations are required. The following items summarize the assumptions made for the ATF study.

- Only the bottom two gimbals of the PPS configuration of figure 1 (azimuth and elevation) are retained. The space required for the magnetic system with roll gimbal does not provide room for the cross-elevation yoke.
- The magnetic system stators are mounted to the elevation gimbal yoke. Exact placement is unimportant for preliminary performance evaluation.
- The control point for the magnetic system is placed as close as possible to the ATF center of gravity.
- Inertial pointing control of the ATF is accomplished with the magnetic actuators. PPS gimbal control is used to orient the actuator stators so as to follow the angular motion of the armature ring.

Figure 3 illustrates a configuration based on these assumptions. The bottom view in the figure looks along the payload X-axis normal to both the line of sight of the payload (Z-axis) and the elevation gimbal axis. It shows two actuators, oriented parallel to the payload axis, which can provide pointing control around the

X-axis and translational isolation along the Z-axis. Pointing control of the elevation yoke around the X-axis (following payload motion on this axis) is achieved using the azimuth gimbal.

The pointing performance of the proposed MIPS was evaluated using a planar three-degree-of-freedom (3 DOF) simulation based on the configuration in figure 3 (the simulation was developed using the MATRIX-x™ design and analyses program from Integrated Systems Inc.). The 3 DOFs in the performance model include:

- Payload inertial angular motion around the payload X-axis, θp
- PPS elevation yoke angular motion around the X-axis, θ_G
- Translational motion of the payload normal to the pointing control axis, Z_p

As figure 3 makes clear, the elevation yoke rotation around the X-axis is determined by the azimuth gimbal rotation and by the PPS base rotation normal to the two gimbal axes, θ_N. This latter parameter is viewed as a disturbance input to the model. The selected planar model was chosen because it allows major disturbance sources, including θ_N, to be evaluated without the complexity and cost of an 8-DOF model.

The functional block diagram of the planar model is given in figure 4. The control loops corresponding to θp, Z_p, and θ_G are labelled inertial pointing loop, isolation loop, and PPS gimbal follow-up loop, respectively. Other details of the model include:

- Two magnetic actuators for inertial pointing and isolation. Actuator models are included to show high-frequency isolation response.
- Interface stiffness and damping (K and B) due to cabling across the azimuth gimbal
- Bearing breakaway friction torque on the azimuth gimbal (T_{fmax}) with linear spring, K_F, up to breakaway
- Effect of payload and PPS rotations (θp, θ_G) and payload and base translation (Z_p, Z_b) on the gap motion (armature-to-stator relative motion) at each actuator.
- Errors in knowledge of payload center of gravity offset from the two actuators; actual R_1 versus assumed R_1; same for R_2.
- Errors in knowledge of gimbal rotation axis offset from the two actuators; ΔR_{B1}, ΔR_{B2}.
- Disturbance inputs due to base translations (Z_b), base rotation around the azimuth gimbal (θ_{AZ}), and base normal axis rotation (θ_N).

Table 1 lists the compensation forms and control bandwidths for the control loops appearing in figure 4. The inertial pointing loop bandwidth limit, 10 rad/s, is conservatively consistent with the assumed first mode frequency of the ATF telescope, i.e. 20 hertz. The form of the isolation compensation is chosen to

produce a very fast ideal high-frequency roll off, (-100 dB/decade). As simulation results show, however, the actuator dynamics limit the frequency range over which the -100-db roll-off is actually produced. Table 2 lists numeric values for several of the model parameters.

POINTING STUDY RESULTS

The primary results of the study conducted with the model of figure 4 relate to the payload pointing errors obtained in response to base acceleration disturbances, Z_b, and base rotational motions, θ_{AZ} and θ_N. In addition to pointing performance results, however, the model was used to define system response characteristics required to specify magnetic actuator force and gap parameters. These characteristics include required control force and actuator gap motion. The three items below summarize these study objectives.

- Define pointing performance for magnetic pointing system (high and low frequency disturbances) as a function of input disturbance level and pointing and isolation bandwidths.
- Define the peak actuator gap motion as a function of input disturbance level and isolation and pointing loop bandwidths.
- Define the control force requirements as a function of input disturbance level.

As described above, pointing performance for the ATF MIPS has been defined by the pointing error generated by single-frequency sinusoidal disturbances (both linear acceleration and base rotations) in the frequency regions below and above 5 hertz. Pointing error levels are determined, using the model of figure 4, by generating the magnitude frequency response curves for the transfer functions from the various disturbance sources to θ_p. At any particular frequency (corresponding to the frequency of the disturbance input), the magnitude of θ_p depends on the magnitude of the disturbance input and the bandwidths of the pointing and isolation control loops.

Figure 5 shows frequency response curves for the $\ddot{Z}_b$ to θ_p transformation. The different curves reflect a variation in pointing loop bandwidth from 5 to 10 rad/s. As indicated in the figure label, the $\ddot{Z}_b$ magnitude used in generating the curves is 0.01g and the isolation bandwidth is 7 rad/s.

The curves of figure 5 show that peak pointing error below 5 hertz is significantly affected by pointing loop bandwidth, while at higher frequencies, pointing error is unaffected by changes in this parameter. By contrast, a variation in isolation bandwidth produces little pointing error change below 5 hertz. This result is due to the fact that pointing error produced by base translational accelerations is proportional to the isolator transmissibility.

Frequency response curves similar to those of figure 5 were also generated for rotational disturbance motions around the azimuth and normal axes. Results from these curves are summarized in Table 3. As indicated, the input disturbance level is 0.3 millrad (or approximately 1 arcmin). For each disturbance and at each

pointing loop bandwidth, the error levels are more than two orders of magnitude below the required specification values.

The major factors influencing payload-to-base relative translational motion, $(Z_B - Z_p)$ in figure 4, and, thus, actuator gap requirements, are isolator bandwidth and level of base translational motion. Frequency response curves for the transformation from $\ddot{Z}_B$ to $(Z_B - Z_p)$, assuming a 0.01g disturbance level and various levels of isolator bandwidth, were generated using the performance model to evaluate these sensitivities. The peak relative motions from these frequency response curves were then used to generate the parameterization curves of figure 6. In this figure, gap motion is plotted against translational disturbance level for various isolation bandwidths. The curves indicate that a 0.5-inch motion limit can be maintained out to 0.02g if the isolation bandwidth is set above 6 rad/s.

The following items summarize the results from the MIPS performance study.

- Low-frequency pointing performance is affected most by pointing loop bandwidth-high frequency performance by the isolator.
- A 10 rad/s pointing bandwidth and 6 rad/s isolation bandwidth satisfy low- and high- frequency pointing requirements for single-axis disturbances <0.018g.
- For the nominal disturbance input level, 0.01g, gap motion is less than 0.5 inch (1.27cm).
- Angular motion disturbances at the 1 arcmin level are insignificant in their effect on pointing error.

MAGNETIC ISOLATION AND POINTING SYSTEM (MIPS) DESIGN

A candidate ATF MIPS, including all potential sources of power and weight, was defined to establish a power, weight, and size budget for such a system. In addition, system reliability was addressed. To place a limit on the peak force required of the magnetic actuators, a peak control force of 80 lbs (356 N), corresponding to a 0.01 translational disturbance acceleration input, was assumed.

The following items summarize the requirements and assumptions imposed on the magnetic system design,

- A 356 N control force can be required in any direction.
- A 34 N.m control torque is required normal to the ATF line of sight.
- Relative motion at any actuator is limited to ±0.5 inch (1.27cm).
- A full ring armature attached to the ATF is required to provide ±200 degrees roll motion.
- A noncontacting roll motor providing 7 N.m (5 ft-lbs) of roll torque is required.

- The magnetic system must fit within an annular region between the PPS and ATF that has a 1.8-meter inside diameter and a 2.5-meter outside diameter.

- The system must provide noncontacting power and signal transfer to the ATF.

Several actuator configurations were considered for the design. The number of actuators in the configuration is important because a large number of actuators implies a small peak actuator force and, thus, a small actuator. A small actuator makes it easier to fit the system into the available radial space. However, each actuator requires separate drive electronics, gap sensors, and flux sensors. Since it is undesirable to make the system any more complicated than necessary, a balance is found between accommodating the radial space limitation and minimizing the number of actuators. While five actuators and a roll motor are adequate for providing ATF control, eight actuators (plus roll motor) were selected for the MIPS, as shown in figures 7, 8, and 9.

A simple model was developed which related peak (of the eight actuators) single actuator force to control force and torque magnitudes and directions to the inclination angle of the armature from the plane of the actuator system. An optimization procedure was implemented to minimize the maximum peak single actuator force and torque. The peak force requirement was determined to be 156 N (35 lbs) at an inclination angle of 52 degrees.

To provide force margin, a peak actuator force of 220 N (or 50 lbs) was chosen for the system. Figure 10 shows the results of the actuator force sizing process carried out for other values of control force. The circled point on the graph corresponds to the nominal configuration values (80 lb, 50 lb or 356 N, 220 N). This places the nominal actuator design in an array of possible actuator force, motion, peak power, and weight options. The curves in the figure relate total system actuator weight (eight actuators) to peak actuator force for different levels of actuator gap motion and single actuator peak power. The curves can be used to determine how an increase in actuator force and motion, or an emphasis on power rather than weight, can be expected to affect the actuator system weight.

The quiescent and peak power requirements for a single actuator were determined to be 5 and 200 watts, respectively. The quiescent power requirement corresponds to the situation where the force command to the actuator is zero and the armature is centered in the actuator gap, i.e. no gap motion. The peak power is required when the actuator is driven to its peak force level while the gap motion is at its limit. In normal operation, an actuator's power requirement, determined by the command force and gap motion, is somewhere in between these extremes. The actuator system's power requirement is, of course, the sum of the individual values.

To define operational power needs of the proposed actuator configuration, a simulation was developed to compute the power for each of the configuration actuators as a function of its commanded force and gap motion. The command forces and gap motions were based on the payload control forces and torques (magnitudes and directions) and on the relative motion between the ATF payload and the actuator stator ring. The maximum operational power was determined to be approximately 450 watts.

Based on the actuator dimensional parameters, a mechanical layout for the proposed magnetic system was generated (figs 7, 8, and 9) that show that the system can fit easily into the available radial space. The cross section in figure 8 also indicates how the actuators might be placed relative to the optical signal coupler channel, the rotary power transformer, and a power-off caging mechanism. The coupler and transformer are described below. The caging mechanism has not been defined. Presumably it would operate on an annular ring and operate when power is lost or on command. A similar cross section of the roll motor placement, with respect to the same armatures used by the pointing and isolation actuators, is shown in figure 9.

ATF roll control is provided by two ac induction motors reacting against the two actuator rings. The motors are placed as indicated in figure 7 to balance disturbance forces produced by the motors. Each motor produces a torque of 3.4 N.m (2.5 ft-lbs).

The rotary transformer designed to transfer power to the ATF from the PPS, is illustrated in figure 8. The majority of the weight is placed on the stator side of the transformer. The transformer is designed to supply 2400 watts peak at 120 volts and 20 kilohertz. The efficiency is 94 percent.

The concept design for signal transfer between the PPS and ATF is also shown in figure 8. The device consists of a reflective channel around the ATF, with optical transmitters (LEDs) and receivers (photodetectors) placed on both rotor and stator sides of the channel. Information is transmitted as sequences of optical pulses, from the ATF to the PPS and vice versa. Multi-information channels can be supported by multiplexing on both sides of the channel.

Support and drive electronics are required for each of the magnetic system components described above: control actuators, roll motors, rotary transformer, and optocoupler. In addition, gap sensor and support electronics are required to support the isolation and PPS follow-up control. Finally, an ATF processor is required to connect all of the functions. All electronics are redundant. Figure 11 is the hardware and signal block diagram which shows this redundancy for the processor, actuator, and roll drive electronics.

Table 4 supplies an estimated breakdown of total system weight and operational power. The values in parentheses refer to changes in power and weight resulting from a change to 100-watt peak power actuators (without a change in motion limit or maximum actuator force). No dimensional layouts were defined to determine whether or not the larger system will actually fit in the available radial space.

The intended 20-year operational life of the ATF experiment mandates that all major electronic components of the MIPS be redundant. A summary of the system component failure rates is provided in Table 5. The redundant electronics components are nonoperational prior to a primary component failure and therefore are assigned a failure rate of 1/10 of the primary failure rate. A single actuator failure is viewed as a system failure. Fewer than eight actuators can be used to control the ATF (with modification to the control software), but the system was sized assuming eight actuators. Thus, an actuator failure may result in unacceptably degraded performance.

The magnetic actuator failure rate listed in table 5, 0.015, assumes a single coil with discrete insulation between coil windings. The failure rate can be improved to 0.00285 by adding redundant coils, but the effect on overall system reliability is very small. A decision to add redundant coils might be made based on the difficulty of exchanging a failed actuator.

CONCLUSION

A magnetic suspension system design, with greater than ±180-degree roll capability, has been generated which will provide the precise pointing and isolation required of the ATF in the presence of a 0.01g Space Station disturbance. The design fits in the available annular space and is estimated to weigh less than 900 kilograms (2000 lbs). Power requirements for the system are dominated by the magnetic actuator and roll motor requirements. Power numbers presented for these systems do not represent the peak possible power for the system. They do, however, represent the anticipated peak operational power. Based on these peak numbers, the total system power requirement is estimated to be < 800 watts. The full redundancy of the system, except actuator coils, provides a reasonable mean time between system failures (defined by system nonoperation or performance degradation).

REFERENCES

1. "Astrometric Telescope Facility: Preliminary Systems Definition Study", NASA TM 89429, Washington, DC: NASA, March 1987.

2. Cunningham, D.C., Gismondi, T.P., and Wilson, G.W.: System Design of the Annular Suspension and Pointing System (ASPS). AIAA Paper 78-1311, Palo Alto, CA, August 1978.

3. Cunningham, D.C., et al: Design of the Annular Suspension and Pointing System. NASA CR-3343, January 1980.

4. Hamilton, B.J.: Laboratory Evaluation of the Pointing Stability of the ASPS Vernier System. NASA CR-159307, June 1980.

5. VanRiper, R.V.: A Precision Pointing System for Shuttle Experiment Payloads. 17th Space Congress, May 1980.

6. Hamilton, B.J.: Experiment Pointing with Magnetic Suspension. SPIE Paper 265-13, Los Angeles Technical Symposium, February 1981.

7. VanRiper, R.V.: High-Stability Shuttle Pointing System. SPIE Paper 265-12, Los Angeles Technical Symposium, February 1981.

8. Hamilton, B.J.: Vibration Attenuation Using Magnetic Suspension Isolation. 1981 Joint Automatic Controls Conference, Charlottesville, VA, June 1981.

9. Hamilton, B.J.: Stability of Magnetically Suspended Optics in a Vibration Environment. SPIE Paper 295-21, San Diego Technical Symposium, August 1981.

10. Hamilton, B.J.: Magnetic Suspension: The Next Generation in Precision Pointing. AAS Paper 82-034, Rocky Mountain Guidance and Control Conference, February 1982.

11. Hamilton, B.J., Samario, E. and Waldman, M.: Talon Gold Control System Architecture. 9th DARPA Strategic Space Symposium, October 1983.

12. Hamilton, B.J. and Keckler, C.: A System for Load Isolation and Precision Pointing. SPIE Advanced Technology Optical Telescopes II, London, England, September 1983.

13. Havenhill, D. and Kral, K.: Payload Isolation Using Magnetic Isolation. AAS Paper 85-014, Rocky Mountain Guidance and Control Conference, February 1985.

14. Hamilton, B.J., Wolke, P. J. and Aldrich, J.: Characterization of VIPS Magnetic Force Actuator. AIAA Paper 85-1988-CP, AIAA Guidance and Control Conference, Snowmass, CO, August 1985.

15. Hamilton, B.J., Andrus, J.H., and Carter, D.R.: Pointing Mount with Active Vibration Isolation For Large Payloads. AAS Paper 87-033, Rocky Mountain Guidance and Control Conference, February 1987.

16. Andrus, J.H.: Cryogenic Magnetic Gimbal Bearing. AIAA Paper 879446, 22nd Intersociety Energy Conversion Engineering Conference, August 1987.

17. Rodden, J.J., Dougherty, H.J., Reschke, L.F., Hasha, M.D., and Davis, L.P.: Line-of-Sight Performance Improvement with Reaction Wheel Isolation. AAS Paper 86-005, Rocky Mountain Guidance and Control Conference, February 1986.

TABLE 1.- SIMULATION MODEL COMPENSATION FORMS

Compensation Description	Form	Open-Loop Bandwidth
Pointing Loop	$\frac{K_R S^2 + K_P S + K_P K_I}{S}$	<10 rad/s
Isolation Loop	$\frac{\frac{\omega_C^3}{32}\left(\frac{S}{(\omega_C/4)} + 1\right)\left(\frac{S}{(\omega_C/8)} + 1\right)}{S\left(\frac{S^2}{(5\omega_C)^2} + \frac{S}{5\omega_C} + 1\right)^2}$	ω_C between 7 and 4 rad/s
Gimbal Follow-up Loop	$\frac{K_{PG} S + K_{PG} K_{IG}}{S\left(\frac{S}{\omega_{LAG}} + 1\right)}$	1 rad/s
Actuator Bandwidth	2nd-order Low Pass	3140 rad/s

TABLE 2.- SIMULATION PARAMETERS

Parameter	Description	Value
θ_P	Payload Interial Angular Motion	
θ_G	Gimbal Angular Motion	
Z_B	Base Translational Motion on Z-Axis	
Z_P	Payload Translational Motion on Z-Axis	
θ_N	Base Rotational Motion Normal Axis	
θ_{AZ}	Base Rotational Motion Azimuth Axis	
K_R	Pointing Compensation Parameters for	10.0
K_P	10 rad/s open-loop crossover	35
K_I		1.7
ω_C	Isolation Compensation, Open Loop Bandwidth	
ω_{LAG}	Gimbal Followup Compensation	4
K_{PG}	Parameters	0.25 * I_{AZ}
K_{IG}		0.25
I_P	Payload Inertia	160,000 kg-m^2
M_P	Payload Mass	3660 kg
I_{AZ}	Azimuth Gimbal Inertia-PPS Only	2050 kg-m^2
L	Actuator Span	1.85 m
$\hat{L}$	Estimate of L	1.85 m
$(R_1 - \hat{R}_1)$	Misknowledge in Payload CG Offset	2 cm
$\Delta R_{B1}, \Delta R_{B2}$	Misknowledge in Location of Magnetic Actuator Force Application Points with Respect to the Gimbal Control Axis	5 cm
EL	Elevation Angle	45°
K	Azimuth Gimbal Interface Stiffness	1700 N•m/rad
B	Azimuth Gimbal Damping Factor	23,000 (N•m-s)/rad

TABLE 3.- ERROR RESPONSE TO 1 ARCMIN AZIMUTH AND NORMAL AXIS ROTATION DISTURBANCES
(Isolator Bandwidth = 5 rad/s)

Pointing Loop Bandwidth (rad/s)	Pointing Error with 1 Arcmin Disturbance			
	θ_{AZ} (arcsec)		θ_N (arcsec)	
	Below 5 Hz	At 5 Hz	Below 5 Hz	At 5 Hz
5	0.0011	0.0001	0.0012	0.0003
7	0.0009	0.0001	0.0011	0.0003
8	0.0009	0.0001	0.0011	0.0003
9	0.0008	0.0001	0.0010	0.0003
10	0.0008	0.0001	0.0010	0.0003

TABLE 4.- MIPS WEIGHT-POWER PREDICTION

Component Description	Max Op Power (W)	Total Weight	
		(lbs)	(Kg)
Actuators (100-W Actuators)	450 (225)	1000 (1400)*	454 (636)
Roll Motors	125	160	72.7
Suspension Electronics (Redundant)	100	120	54.5
Processor	16	32	14.5
Optical Coupler	16	40	18.2
Roll Motor Electronics (Based on 60% Roll Motor operation)	80	50	22.7
Structure	-	225 (325)	103.3 (147.7)
Rotary Transport	(94% Efficient)	310	140.9
System Total (with 100-W Actuators)	787 (562)	1937 (2437)	880.5 (1107.7)

* Power and weight values corresponding to the use of magnetic actuators requiring 100 watts peak power.

TABLE 5.- MIPS ESTIMATED RELIABILITY

Component Description	Quantity	Failures per million hours of operation (λ)			
		Individual	Total	Primary Electronics	Redundant Electronics
MAGNETIC ACTUATOR ELECTRONICS				8.29	0.829
Drive Electronics	8	0.49	3.92		
Standby Electronics	1	3.86	3.86		
Flux Sensor	8	0.002	0.016		
Gap Sensor	8	0.062	0.496		
MAGNETIC ACTUATOR	8	0.015		0.12	
ROLL MOTOR	2	0.03		0.06	
ROLL MOTOR ELECTRONICS				4.64	0.464
Drive Electronics	2	1.05	2.10		
Standby Electronics	1	2.29	2.29		
Gap Sensor	4	0.062	0.25		
OPTOCOUPLER	8	0.3		2.40	0.24
COMPUTER	1	2.4		2.40	0.24
ROTARY TRANSFORMER	1	0.06		0.06	
TOTAL MTBF				17.97	
Probability of Success					
5-year mission				0.455	0.905
10-year mission				0.207	0.711

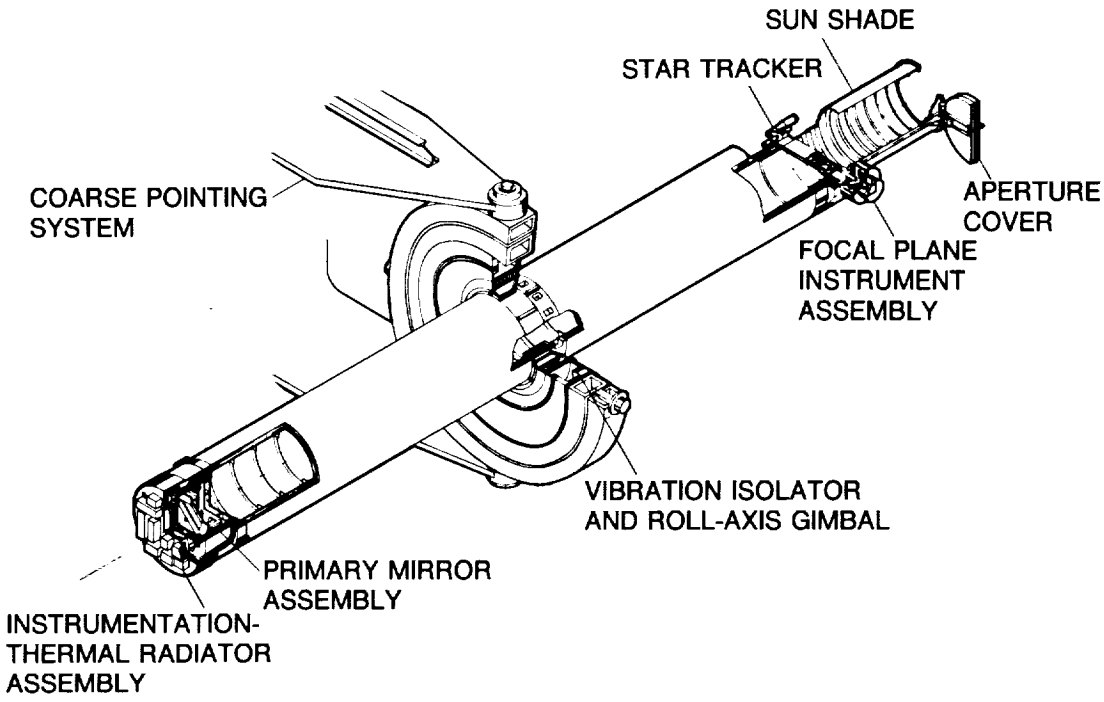

Figure 1. Mission and System Description and Requirements ATF/CPS Mounting Interface Concept

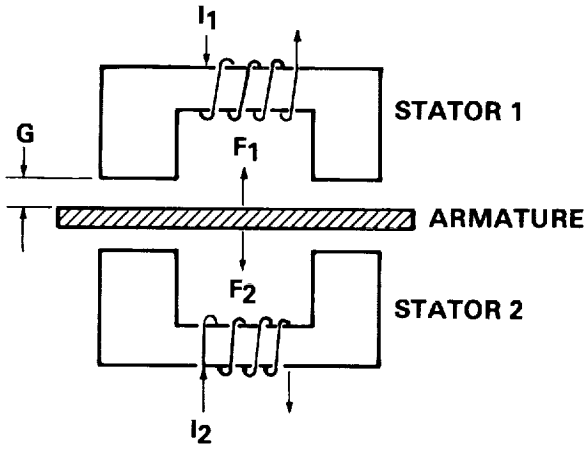

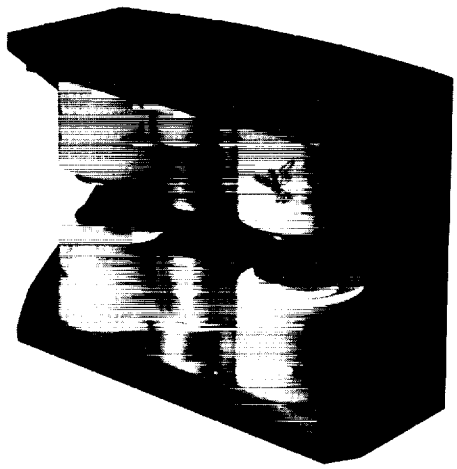

- Attractive Force F_1 and F_2
- F Insensitive to Armature Rotation and Cross Axes Translation
- Armature Isolated From Stator Disturbance Forces

- $F \sim I^2$
- $F \sim G^{-2}$
- Moving Armature Is Passive

Figure 2. Magnetic Actuator

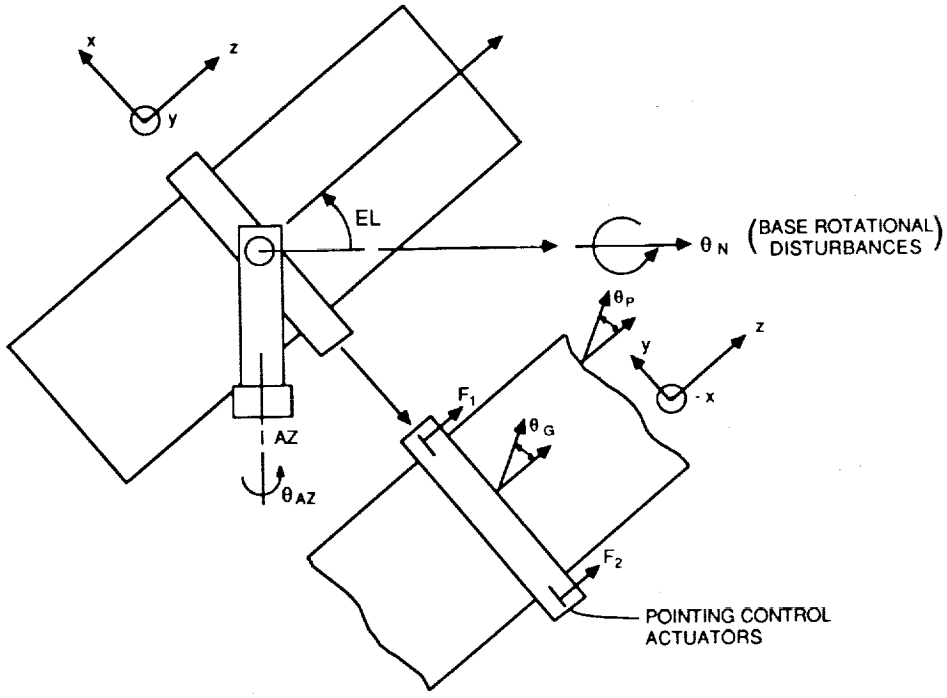

Figure 3. ATF Magnetic Isolation and Pointing Physical Configuration

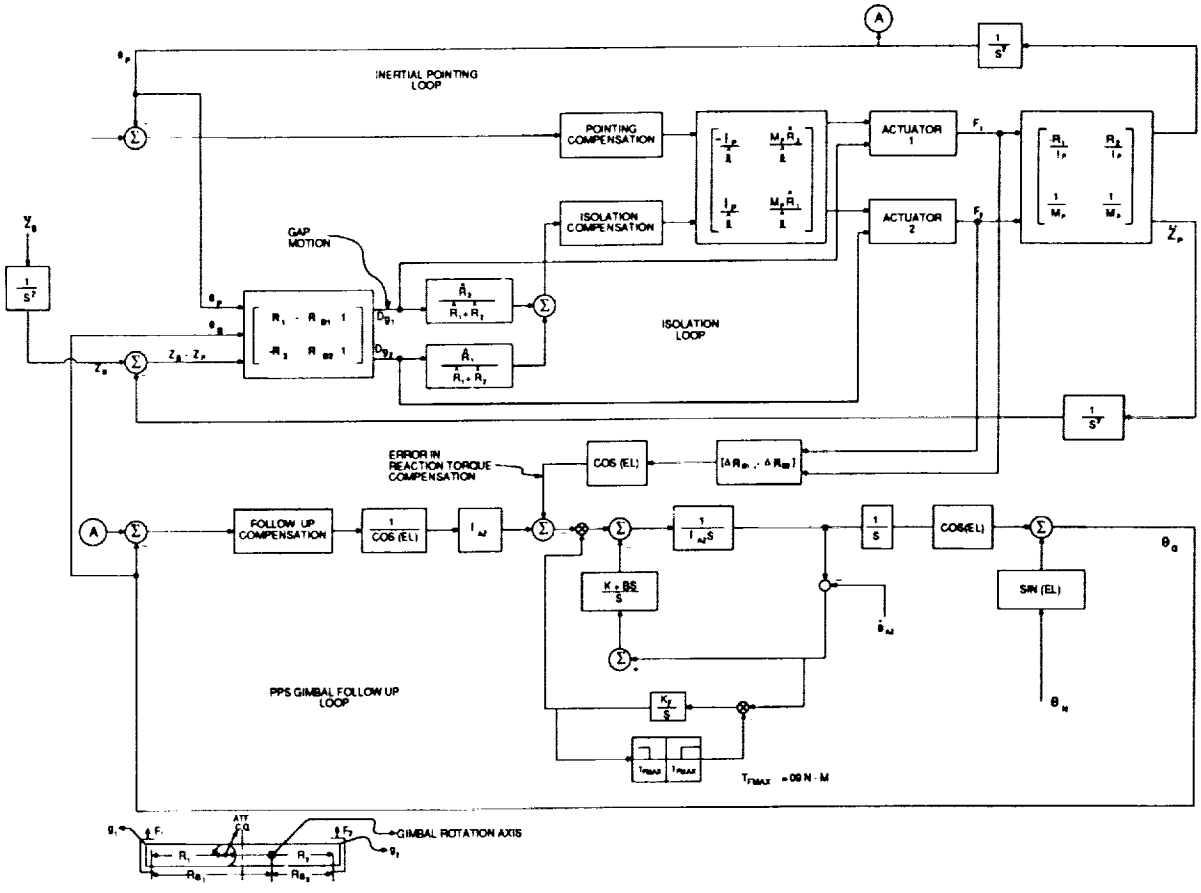

Figure 4. Magnetic Isolation and Pointing Block Diagram

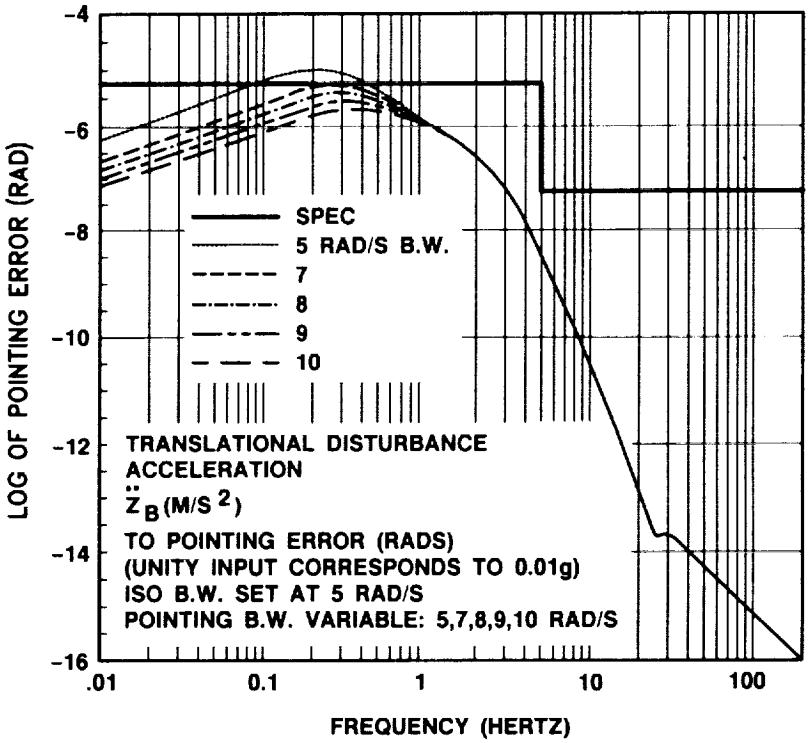

Figure 5. Frequency Response Curves, Translational Disturbance Acceleration to Pointing Error - Isolation Bandwidth = 5 rad/s

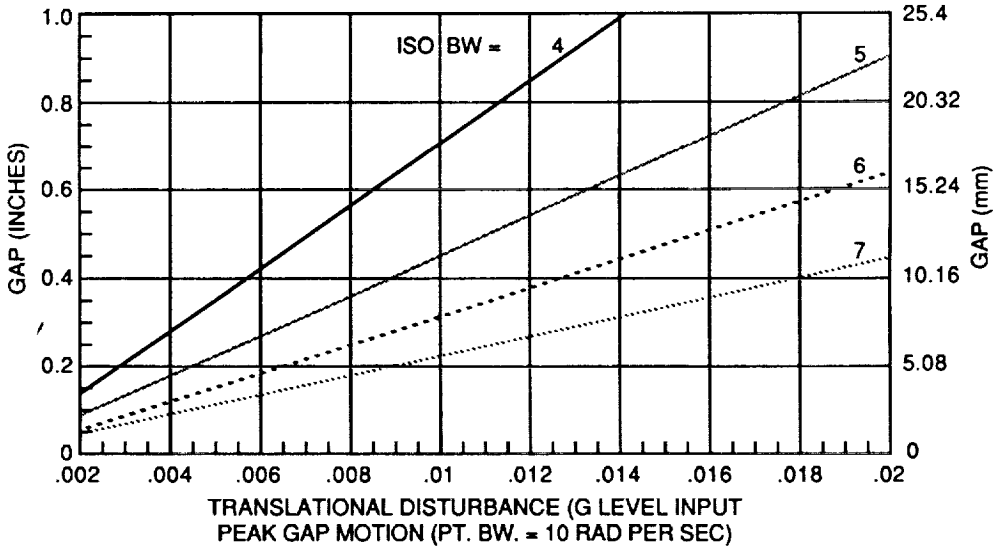

Figure 6. Actuator Gap Motion Requirements Versus Linear Acceleration Disturbance Level, Isolation Bandwidth-Variable

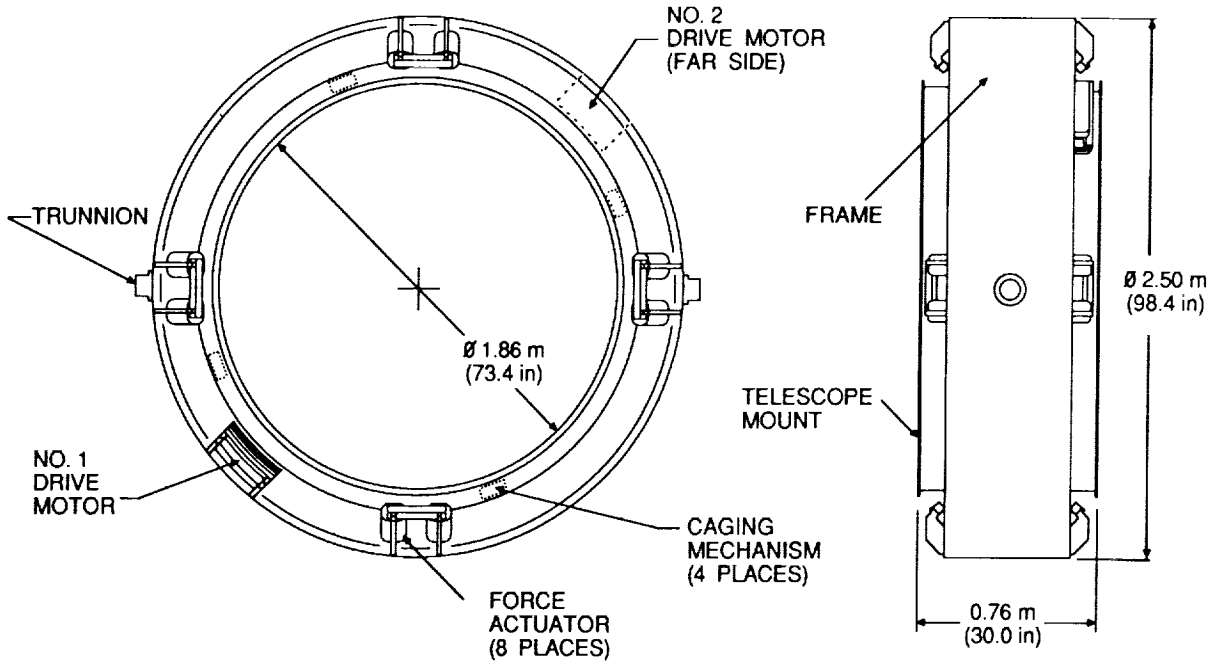

Figure 7. Actuator Layout

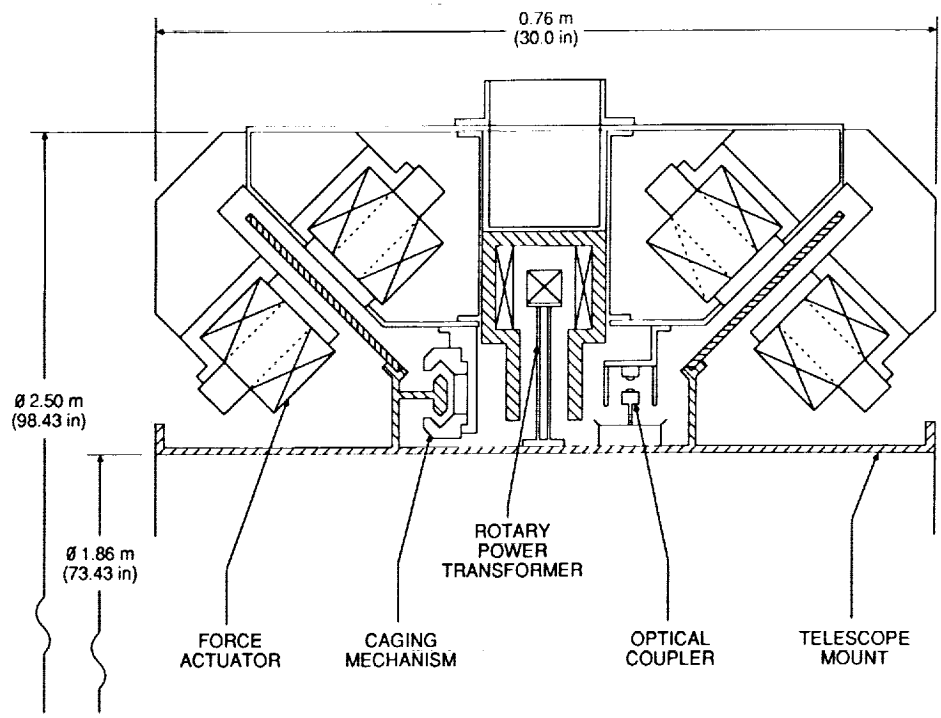

Figure 8. Actuator Cross Section

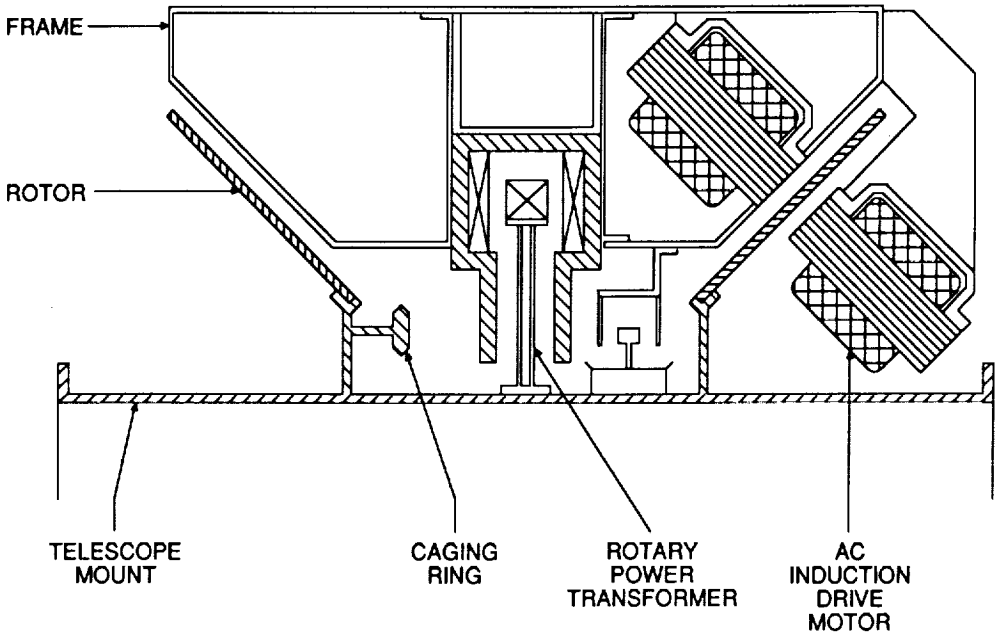

Figure 9. Roll Motor Cross Section

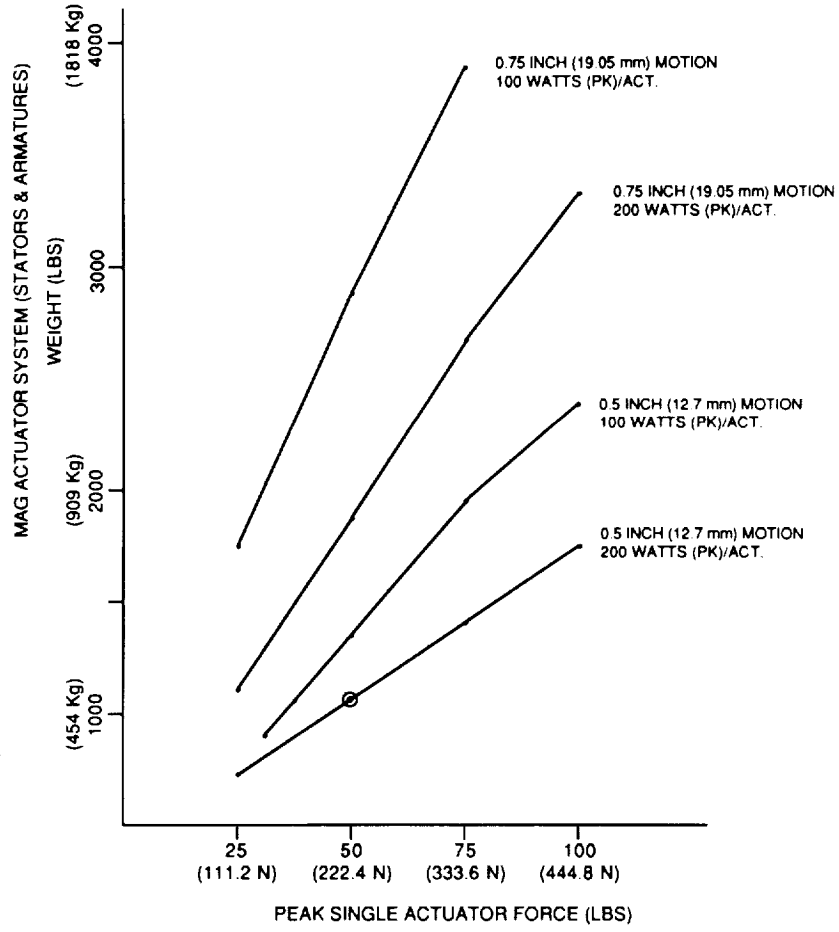

Figure 10. Actuator System Weight Versus Actuator Force

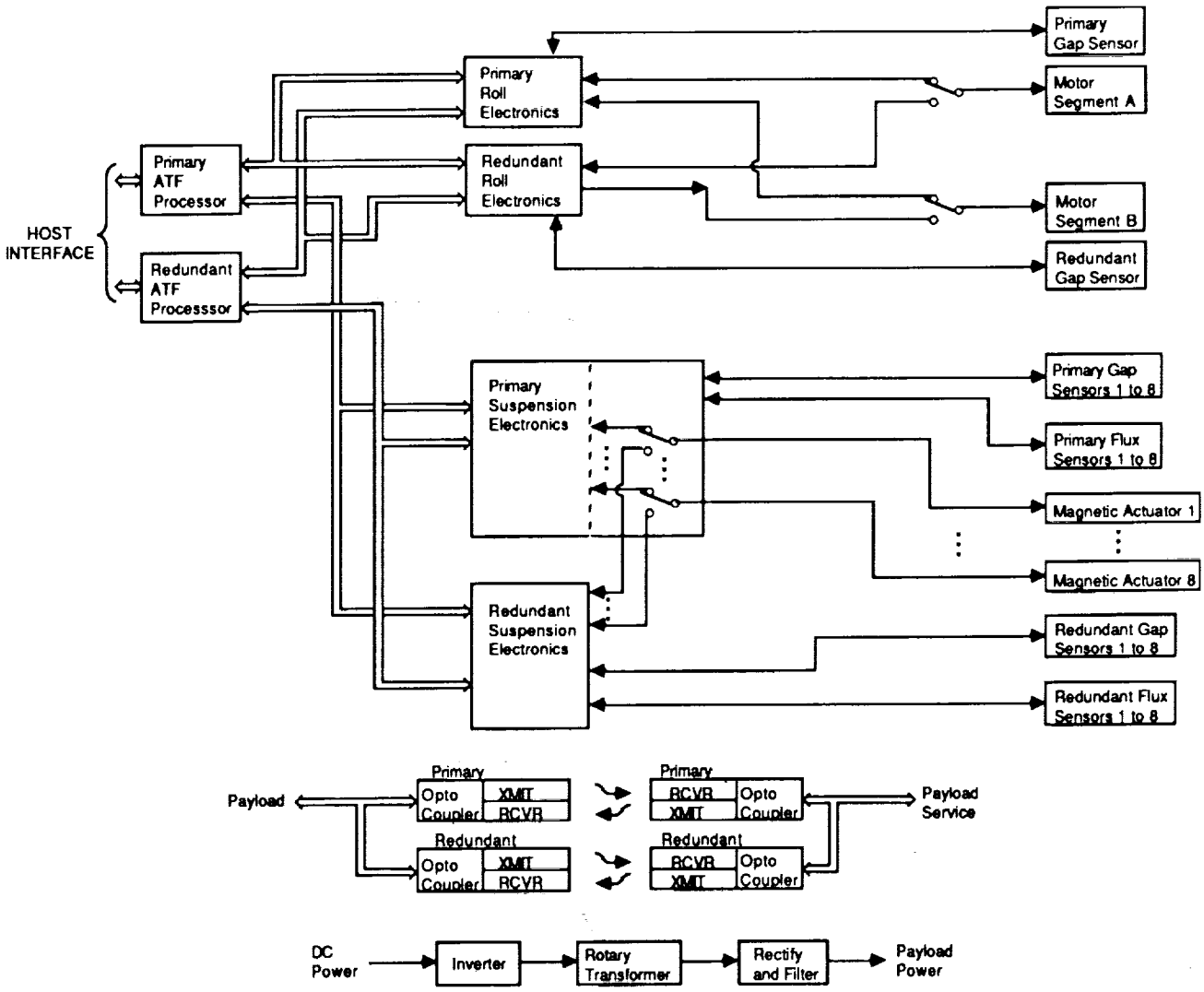

Figure 11. ATF MIPS Equipment